



Journal of Rehabilitation in Civil Engineering

Journal homepage: <https://civiljournal.semnan.ac.ir/>

## A Simple Solution for Estimating the Smear Effect Permeability Ratio Using Finite Element Method

Rufaizal Che Mamat <sup>1,\*</sup> ; Azuin Ramli <sup>1,\*</sup> ; Sri Atmaja P. Rosyidi <sup>2</sup>

1. Centre of Green Technology for Sustainable Cities, Department of Civil Engineering, Politeknik Ungku Omar, Jalan Raja Musa Mahadi, Ipoh 31400, Perak, Malaysia

2. Department of Civil Engineering, Universitas Muhammadiyah Yogyakarta, Jalan Brawijaya, Bantul, Yogyakarta, 55183, Indonesia

\* Corresponding author: [rufaizal.cm@gmail.com](mailto:rufaizal.cm@gmail.com) (R.C.M.), [azuin.ramli@puo.edu.my](mailto:azuin.ramli@puo.edu.my) (A.R.)

### ARTICLE INFO

#### Article history:

Received: 15 November 2022

Revised: 06 May 2023

Accepted: 05 July 2023

#### Keywords:

Soft soil;

Smear zone;

Road embankment;

Prefabricated vertical drains;

Finite element method.

### ABSTRACT

The installation of a vertical drains system beneath the embankment results in enhanced soil consolidation in soft soil. This article explores the behaviour of soft soil stabilized with prefabricated vertical drains (PVDs) beneath embankments through finite element analysis. A multi-drain analysis, which varied the smear effect permeability ratio using both equivalent and plane strain models, was performed. Back-calculation of the permeability ratio of the smear effect is employed to adjust the model parameters. The analytical formulation employed the Cam-clay concept in combination with the smear effects. The study revealed that PVDs installation in the soft soil beneath the embankment increased the settlement rate and improved pore water pressure dissipation. Accurate prediction requires the estimation of the equivalent horizontal permeability using appropriate values of the smear effect permeability ratio. Incorporating the smear effect into the numerical analysis of vertical drains improved prediction accuracy. The article proposes a new approach for estimating the smear effect permeability ratio for soft soil stabilized with PVDs.

E-ISSN: 2345-4423

© 2024 The Authors. Journal of Rehabilitation in Civil Engineering published by Semnan University Press.

This is an open access article under the CC-BY 4.0 license. (<https://creativecommons.org/licenses/by/4.0/>)

#### How to cite this article:

Che Mamat, R., Ramli, A., & P. Rosyidi, S. A. (2024). A Simple Solution for Estimating the Smear Effect Permeability Ratio Using Finite Element Method. *Journal of Rehabilitation in Civil Engineering*, 12(1), 34-46.

<https://doi.org/10.22075/jrce.2023.28956.1751>

## 1. Introduction

Prefabricated vertical drains (PVDs) are widely used today to improve soft soils, where they can accelerate the soil consolidation process by increasing water drainage rates. Soft soils are usually characterized by low shear strength and high compressibility, which can result in the settlement and instability of road embankments [1]. It is designed to improve the performance of soft soils by creating channels for water to flow quickly and effectively. Also, this approach can save costs and shorten the installation time [2]. Based on this advantage, many previous studies have praised this method for improving the properties of soft soil. In principle, PVDs installed in soft soil provide a path for pore water to flow rapidly out of the soil. This process accelerates the consolidation of the soil, which can increase the stability and strength of the soil, in turn providing a more stable foundation for the road embankment [3]. Since Kjellman [4] introduced this method, many studies have been performed on the soft soil smear effect. The smearing effect is due to the installation of the PVDs into the soft soil with the mandrel, and this will create a smear zone around the vertical drain, as shown in Fig. 1. In this zone, the condition of the soil has been disturbed, which results in a change in the moisture content in turn reducing the permeability of the surrounding domain. [5–7].

The smearing effect for analytical and numerical analysis has been extensively studied over the past four decades. The first method for analyzing axisymmetric vertical drains and solving radial drains consolidated analytically was introduced by Barron [9].

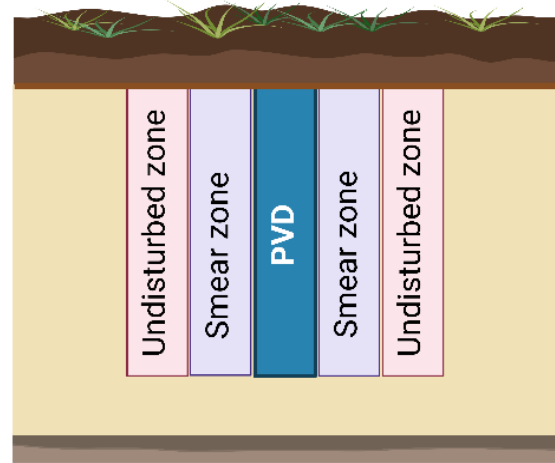


Fig. 1. Smear zone in plane strain [8].

This method continued to be developed by many researchers until the existence of the computing era with the emergence of numerical methods. Since plane strain analysis in numerical methods was introduced, some researchers claim that the permeability ratio of the smear effect ( $k_h/k_s$ ) is the main factor affecting the consolidation rate in the assessment of ground foundation settlement [10–13]. Due to vertical drains being axisymmetric, equivalence must be performed in plane strain. However, this ratio is difficult to estimate accurately because it depends on the permeability rate in the field, which is not consistent due to water flow in vertical drains. Furthermore, the smear zone is also affected by the well resistance and transmissivity of the drainage mat. Despite efforts from other researchers to formulate based on the literature, the proposed value range is 1 to 6 [6,14].

Single drain analysis has been performed previously by modelling soil behaviour along the embankment centreline. However, the analysis of multi-drains caused by varying gravity loads along the embankment width to accurately predict settlement is limited. Thus,

a simple solution is proposed to estimate the permeability ratio of the smear effect presented in this study. The proposed solution is a procedure that combines back-calculation techniques, and numerical analysis is presented. A multi-drain plane strain model was developed using PLAXIS 2D [15] to simulate the settlement and excess pore water pressure under the embankment. Comparative analysis between the estimated and measured is performed based on the back-calculation results to verify the smear effect permeability ratio.

## 2. Site description, construction procedure and field monitoring

This study is based on an extension road construction project in Yan, Kedah, Malaysia, which involves 18.2 km, as shown in Fig. 2. The site of this project is close to the sea in the Strait of Melaka, which is located in a low flood plain. Due to this project is built on soft ground that has a high-water table, improvement techniques using PVDs are used and installed in a triangular formation. In this study, numerical analysis was performed based on data at CH 1233.



Fig. 2. Location of site study.

In order to reinforce the soft soil surface, a sand cushion with a thickness of 0.5m was used and divided into two layers of 0.3m and 0.2m thickness. Geotextiles were placed between the layers to improve the soil shear strength during preloading. PVDs with dimensions of 100mm width and 4.5mm thickness were installed to the subsoil at a distance of 1m and a depth of 14m, with a manufacturer-provided discharge capacity and a tensile strength greater than 1500 m<sup>3</sup>/year and 2.8 kN, respectively. Nonhomogeneous soil was used as the fill embankment and compacted with machinery to construct the embankment, which had a side slope of 1V:1H and a top width of 11m.

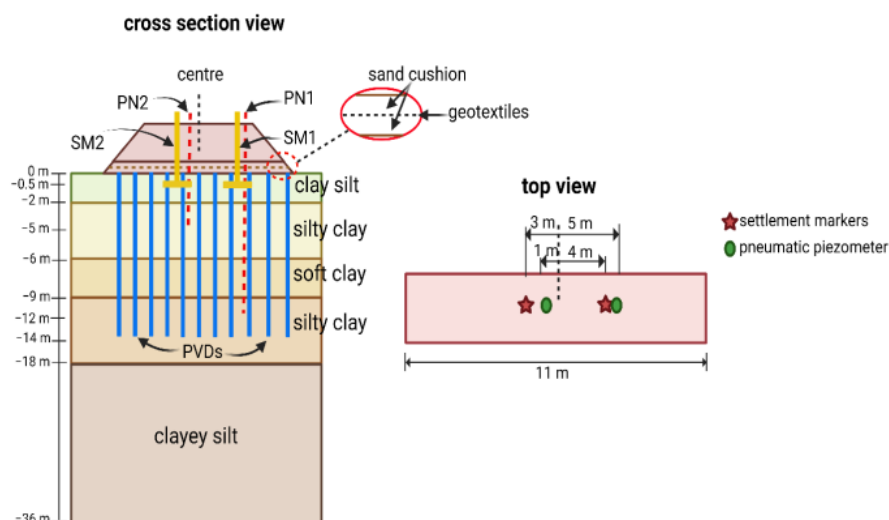


Fig. 3. Field instrumentation layout.

Heavy field instrumentation, including settlement and pore water pressure, was installed and monitored using settlement markers and pneumatic piezometers, as shown in Fig. 3. A total of two settlement markers were installed in two locations (SM1 and SM2), where marker posts were driven into the ground at a depth of 0.5m using a hydraulic driver. A flat reference plate is attached to the top of the marker post and fastened with bolts. Data readings are taken for 177 days after the PVDs installation was completed using survey instruments and compared with initial readings to determine the settlement rate. Pneumatic piezometers are installed vertically and securely in two different borehole locations (PN1 and PN2) where the groundwater level can be easily monitored. The borehole is filled with bentonite pellets to prevent any movement of groundwater around the piezometer. Regular readings are taken on pneumatic piezometers to monitor groundwater levels during and after road construction. The readings taken using the data logger are compared to the initial readings to

determine any changes in the groundwater level.

### 3. Subsoil conditions

Prior to the commencement of the construction, a sequence of field exploration programs were implemented to evaluate the prevailing soil conditions at the construction site. The resultant embankment was erected atop a stratigraphy of five distinct layers of soft soil. The initial layer comprises clay silt, extending to a depth of 2 meters, succeeded by a layer of silty clay, 4 meters in thickness. Further down, a layer of soft clay, measuring 3 meters in depth, underlies the aforementioned silty clay layer. The fourth layer is composed of silty clay, extending to a depth of 4 meters, followed by a deep layer of clayey silt, measuring 18 meters in thickness. The water table exists at a depth of 2.3 meters below the ground surface. The physical and mechanical characteristics of the soil were examined, both on-site and in the laboratory, as detailed in Table 1. The consolidation test, which is utilized to determine the soil's permeability ( $k$ ), was conducted.

**Table 1.** Soil physical and mechanical properties.

Soil strata	USCS	N-SPT	$e_0$	$G_s$	$C_c$	$p_c$ (kPa)	$k$ (m/year)
Clay silt	ML	1	2.17	2.54	0.983	21	0.061
Silty clay	CH	2	2.33	2.54	1.02	18	0.074
Soft clay	CH	1	2.67	2.52	0.952	21	0.056
Silty clay	CH	14	3.00	2.52	1.07	17	0.052
Clay silt	ML	39	3.09	2.51	0.944	22	0.045

Note:  $e_0$  = initial void ratio;  $G_s$  = specific gravity;  $C_c$  = compression index;  $p_c$  = pre-consolidation pressure;  $k$  = coefficient of permeability

### 4. Numerical modelling

In the previous study, finite element method (FEM) is often employed for numerical modelling [16], simulating [3], analysing [13] performance PVDs improvement techniques

because it is user-friendly and simple. Thus, in this study, the FEM with commercial software PLAXIS 2D version 8.2 was selected to simulate the subsoil behaviour of the embankment and compared it with the field measurement. The plane strain condition, 15-

node triangular elements with medium mesh, was adopted in the FEM simulation. The model was developed with subsoil 37m below ground level and 15m horizontally from the embankment centre. The boundary conditions and drainage are standard fixities where the lateral vertical edges use horizontal fixity, and the bottom edge is assumed to be no horizontal and vertical movements.

#### 4.1. Model parameters

The fill material of the embankment and sand cushion are simulated using the linearly elastic perfectly plastic Mohr-Coulomb (MC) model, while the subsoil, which includes soft soils, is modelled using the soft soil model (SS). These models have been widely adopted by researchers for numerical simulations of embankments constructed on soft soils [17]. The MC model is straightforward and requires five parameters, including cohesion ( $c$ ), internal friction angle ( $\phi$ ), Poisson's ratio ( $\nu$ ), effective Young's modulus ( $E_{ref}$ ), and dilatancy angle ( $\psi$ ). The values of  $\nu$  and  $E_{ref}$  are determined according to the elastic constants table of various soils proposed by AASHTO [18]. Additionally, the two parameters required in the SS model are obtained from consolidation test data, namely the modified swelling index ( $\kappa^*$ ) and modified compression index ( $\lambda^*$ ). The permeability coefficient of the fill material of the embankment and sand cushion is 1m/day. The geotextile layer is simulated at the height of 0.3m in the cushion sand, and in PLAXIS 2D [15], the geotextile is characterized by two crucial parameters, tensile element (EA) and soil shear resistance with reinforcing material ( $R$ ). For this study, the model adopted  $R = 1.0$ , and EA is set at 2500 kN/m. The model parameters utilized in this research are presented in Table 2.

The parameters in Table 2 are calculated based on the physical and mechanical characteristics in Table 1. The soil unit weight can be estimated using the N-SPT by using Meyerhof's equation. The equation is as follows:

$$\gamma = \left( \frac{N_{60} - 15}{30} \right) + \gamma_{sat} \quad (1)$$

where  $\gamma$  is the soil unit weight ( $\text{kN/m}^3$ ),  $N_{60}$  is the corrected N-SPT value for 60% energy transfer and  $\gamma_{sat}$  is the saturated soil unit weight ( $\text{kN/m}^3$ ). The unit weight of soil saturation is calculated based on the Skempton-Bjerrum equation as presented in Eq (2).

$$\gamma = \frac{(5.5 + 0.0055N_{60})}{1 + e_0} \quad (2)$$

where  $\gamma_{sat}$  is the saturated soil unit weight ( $\text{kN/m}^3$ ) and  $e_0$  is the initial void ratio.

Shear strength parameters that include cohesion ( $c$ ) and soil friction angle ( $\phi$ ) are determined based on the results of triaxial tests in the laboratory. The triaxial test is used to determine Poisson's ratio ( $\nu$ ) using the formula presented in Eq (3).

$$\nu = \frac{\delta_{strain}}{\delta_{axial}} \quad (3)$$

where  $\delta_{strain}$  is the lateral strain and  $\delta_{axial}$  is the axial strain. The effective Young's modulus ( $E_{ref}$ ) of soil can be determined using the results of an oedometer test and the following in Eq. (4):

$$E_{ref} = \frac{(1 + e_0)(\sigma_1 - \sigma_3)}{\delta_1 - \delta_3} \quad (4)$$

where  $e_0$  is the initial void ratio of the soil,  $\sigma_1$  is the effective vertical stress at the end of primary consolidation,  $\sigma_3$  is the effective horizontal stress at the end of primary

consolidation,  $\delta_1$  is the axial strain at the end of primary consolidation,  $\delta_3$  is the radial strain at the end of primary consolidation. In order to determine the dilatancy angle of soil using the shear test results, the following Eq. (5):

$$\tan \psi = (\tau' / \sigma'_n) - (\tau / \sigma) \quad (5)$$

where  $\psi$  is the dilatancy angle,  $\tau'$  is the effective shear stress,  $\tau$  is the total shear stress,  $\sigma'_n$  is the effective normal stress in the direction of the shear plane and  $\sigma$  is the total normal stress in the direction of the shear plane. The modified oedometer test was used to determine the modified swelling index of soil as presented in Eq. (6).

$$\kappa^* = (\Delta V / V) / (\Delta \sigma) \quad (6)$$

where  $\Delta V / V$  is the change in volume of the soil sample relative to its initial volume and  $\Delta \sigma$  is the change in applied stress. The modified compression index ( $\kappa^*$ ) of soil is typically determined from the slope of the strain-logarithm of time curve in the secondary compression region. The formula to calculate the modified compression index is as in Eq. (7).

$$\lambda^* = (\Delta \delta / \Delta \log t) / \sigma \quad (7)$$

where  $\Delta \delta$  is the change in strain over the logarithm of time,  $\Delta \log t$  is the change in time and  $\sigma$  is the effective stress.

**Table 2.** Model parameters.

Soil strata (Model)	Type	$\gamma_{unsat}$ (kN/m <sup>3</sup> )	$\gamma_{sat}$ (kN/m <sup>3</sup> )	$\nu$	$E_{ref}$ (kN/m <sup>2</sup> )	$c_{ref}$ (kN/m <sup>2</sup> )	$\Phi$ (°)	$\Psi$ (°)	$\lambda^*$	$\kappa^*$
Fill material (MC)	Drained	16.5	-	0.3	15,000	10	20	0	-	-
Sand cushion (MC)	Drained	17.0	-	0.3	20,000	0	30	0	-	-
Clay silt (SS)	Undrained	13.1	13.6	0.15	-	75	0	0	0.100	0.023
Silty clay (SS)	Undrained	13.3	13.8	0.15	-	43	0	0	0.116	0.027
Soft clay (SS)	Undrained	13.6	14.0	0.15	-	43	0	0	0.113	0.026
Silty clay (SS)	Undrained	14.0	14.5	0.15	-	11	0	0	0.133	0.031
Clay silt (SS)	Undrained	14.5	15.8	0.15	-	10	0	0	0.135	0.031

Note:  $\gamma_{unsat}$  = unsaturated unit weight;  $\gamma_{sat}$  = saturated unit weight;  $c$  = cohesion;  $\phi$  = internal friction angle;  $\nu$  = Poisson's ratio;  $E_{ref}$  = effective Young's modulus;  $\psi$  = dilatancy angle;  $\kappa^*$  = modified swelling index;  $\lambda^*$  = modified compression index.

#### 4.2. Equivalent plane strain modelling

The axisymmetric vertical drains consolidation theory is widely accepted in foundation engineering due to its simplicity. In order to model the nearly plane-strain soil in the drainage system's area, a condition of axial symmetry is used for the 2D model. Hird et al. [19] proposed an Eq. (8) for the equivalent permeability under in-plane strain, which includes the width ( $B$ ) and diameter ( $D_e$ ) of the plane strain unit cell, the factor of the vertical

drain geometry ( $\mu$ ), and the horizontal permeability of the subsoil ( $k_h$ ).

$$k_{hpl} = \frac{2}{3} \left( \frac{B^2}{D_e^2} \right) \left( \frac{1}{\mu} \right) k_h \quad (8)$$

The factor of the vertical drain geometry is determined by the ratio of the diameter of the unit cell and drainage ( $n$ ), the ratio of the diameter of the smear zone and drainage ( $s$ ), as well as the horizontal permeability in the smeared zone ( $k_s$ ), and the diameters of the

smear zone and vertical drain ( $d_s$  and  $d_w$ , respectively). This parameter can be estimated using Eq. (9) as below:

$$\mu = \ln\left(\frac{n}{s}\right) + \left(\frac{k_h}{k_s}\right) \ln(s) - 0.75 \quad (9)$$

For triangular patterns of PVDs installation, the diameter of the unit cell ( $D_e$ ) is determined by Eq. (12). If neglecting the effect of the smear, the equivalent horizontal permeability is given by Eq. (10), which uses the parameters summarized in Table 3 and the equivalent drain diameter ( $d_w$ ) proposed by Rixner et al. [20] in Eq. (11). The diameter of the smear zone ( $d_s$ ) can be calculated using the equations proposed by Hird & Moseley [21], and is relevant for the installation of PVDs in soft ground where discharge capacity ( $q_w$ ) is less than  $100 \text{ m}^3/\text{year}$  [22].

$$k_{hpl} = \frac{0.67k_h}{(\ln(n) - 0.75)} \quad (10)$$

$$d_w = \frac{(w+t)}{2} \quad (11)$$

$$d_e = 1.05d \quad (12)$$

In Eq. 13, Hird & Moseley [21] has introduced a solution to estimate the diameter of the smear zone. Based on this equation,  $w$  and  $t$  are width and thickness of PVDs respectively.

$$d_s = 1.6d_w \quad (13)$$

In this study, the solution proposed by Hird et al. [19] was used with different smear effect permeability ratios ( $k_h/k_s = 1, 3$  and  $6$ ) based on the literature to estimate the equivalent permeability. A perfect (ideal) drain should have a large  $q_w$  exceeding  $100 \text{ m}^3/\text{year}$  [20]; however, in this study, the well-resistance effect was neglected as the discharge capacity of PVDs is  $120 \text{ m}^3/\text{year}$ .

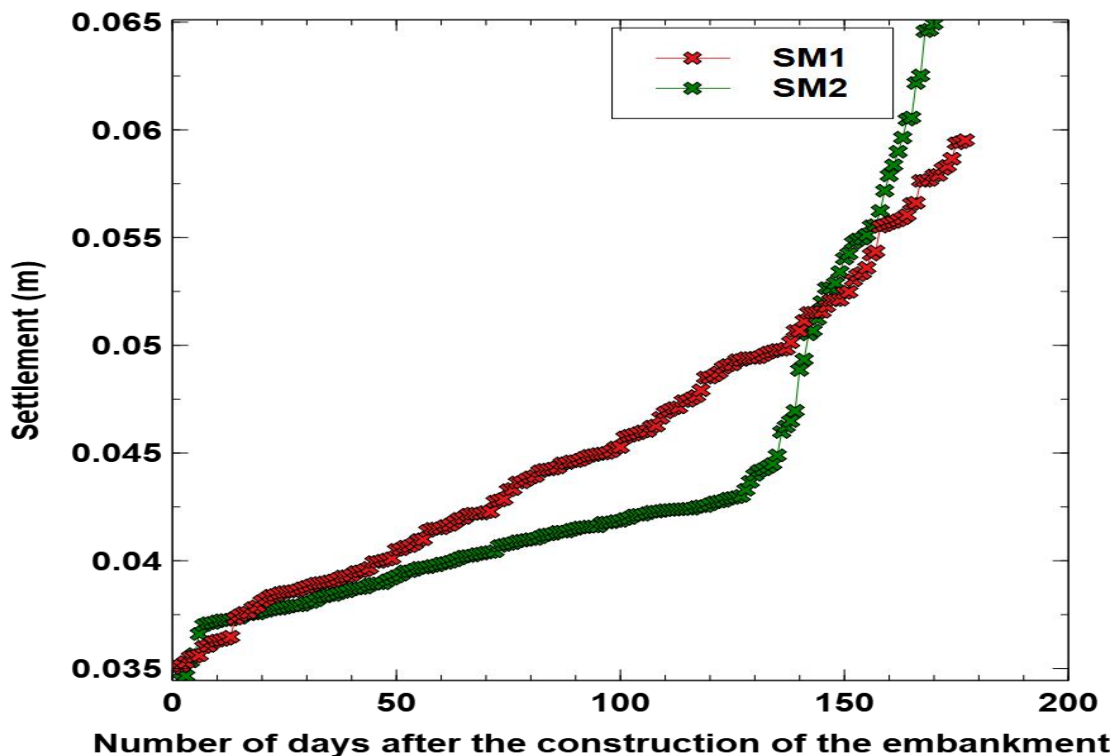


Fig. 4. Settlement at the locations of settlement makers.

## 5. Results and discussion

The settlement data obtained from the settlement markers is presented in Fig. 4, with time as the variable. The figure depicts that the settlement was consistent along the longitudinal axis of the embankment. The settlement markers measurements provide confirmation of the embankment settling under plane strain conditions.

Figure 5 displays the excess pore pressures observed by the pneumatic piezometers, which are positioned at the mid-point of the vertical drain grid to measure the maximum excess pore pressure. The groundwater level was found to have increased because the site became flooded over time throughout the construction work.

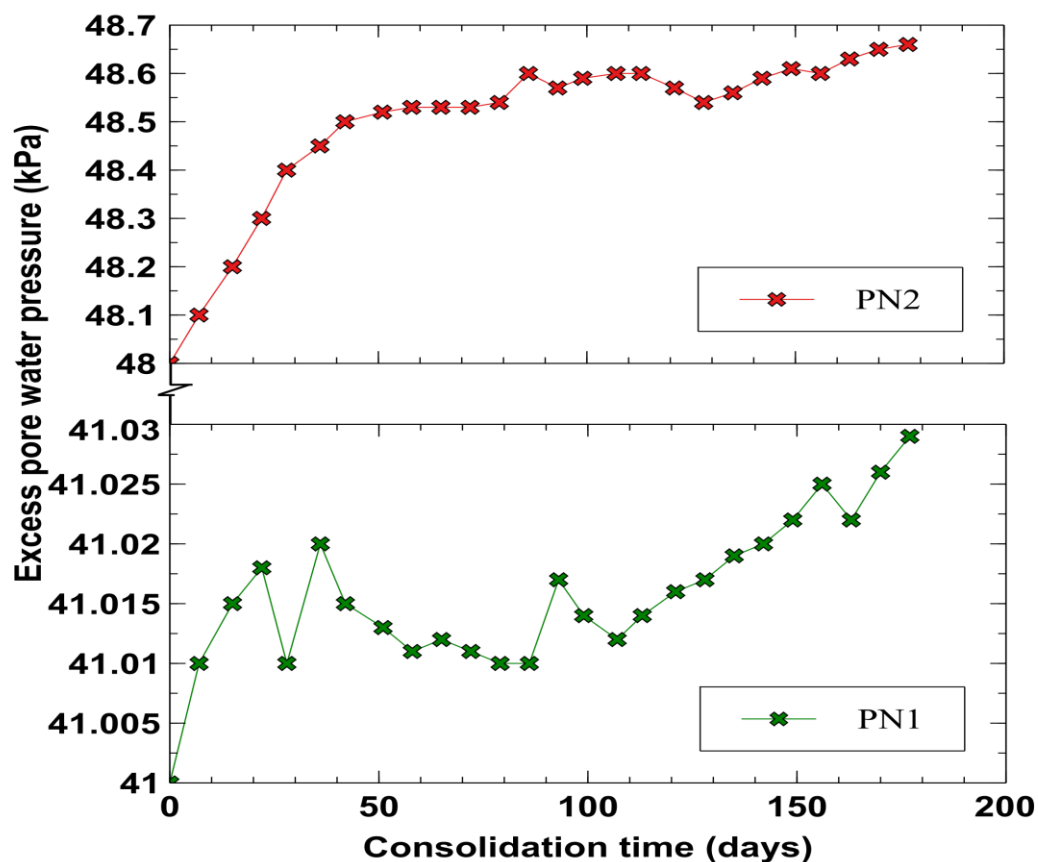


Fig. 5. Excess pore water pressure from pneumatic piezometer.

In the numerical analysis, the embankment was modelled with a static vertical load applied to the top boundary. The excess pore water pressure of the drainage boundary is set to zero to simulate perfect drainage conditions. The analysis carried out involves modelling multi-drains to predict settlement more accurately and reliably. Two types of drain conditions were performed in the simulation,

including perfect drains and smear effect drains. Back-calculation of the permeability ratio of the smear effect is done by adjusting the model parameters until the results of the simulated settlement are consistent with the measured settlement data. The accuracy of the obtained permeability ratio is verified by comparing simulated and measured excess pore water pressure data. For this purpose, the



smear effect permeability ratio ( $k_h/k_s$ ) was validated based on the comparison results between the predicted and measured.

Figures 6 and 7 show the predicted accuracy of the settlement for SM1 and SM2 with varying smear effect permeability ratios ( $k_h/k_s = 1, 3$  and  $6$ ). It is apparent that the numerical models developed in good agreement with  $R^2 \geq 0.9$ . Surprisingly, the numerical model with  $k_h/k_s = 6$  was found that  $R^2$  values were similar (0.9921) in SM1 and SM2, although a numerical model with  $k_h/k_s = 3$  in SM2 found that  $R^2$  values were high (0.9934). Due to the model with  $k_h/k_s = 6$  has a good reliability prediction accuracy; then this value was used in the analysis of the behaviour of soft soil stabilized with PVDs beneath embankment against multi-drain.

The settlement profile predicted from the ground surface of 7 m depth is shown in Fig. 8 for SM1 and SM2. The analysis involves only the smear effect. As expected, maximum settlement occurs on the soft ground surface. These results match those observed in earlier studies [23]. The change in the ground

settlement that depends on time becomes negligible from the surface and approaching the base. It was also found that the total settlement decreased significantly from the ground surface to 2m depth and demonstrated no difference afterwards. The largest total settlement is associated with SM2, mainly due to its location near the embankment centre compared to SM1. The predicted and measured excess pore pressures in PN1 and PN2 are compared and presented in Fig. 9. In this study, the predicted negative excess pore pressure was generated in the soft ground. The excess pore pressure predicted and measured shows an increasing trend for six months of construction. As expected, the predictions of smear effect drain are in good agreement compared to the perfect drain underestimated with measured. Moreover, the excess pore pressure data predicted and measured in PN1 were plotted show considerably poor compared to PN2, which has a smooth curve graph. This may be due to the proximity of PN1 to the embankment toe, which contributes to data uncertainty.

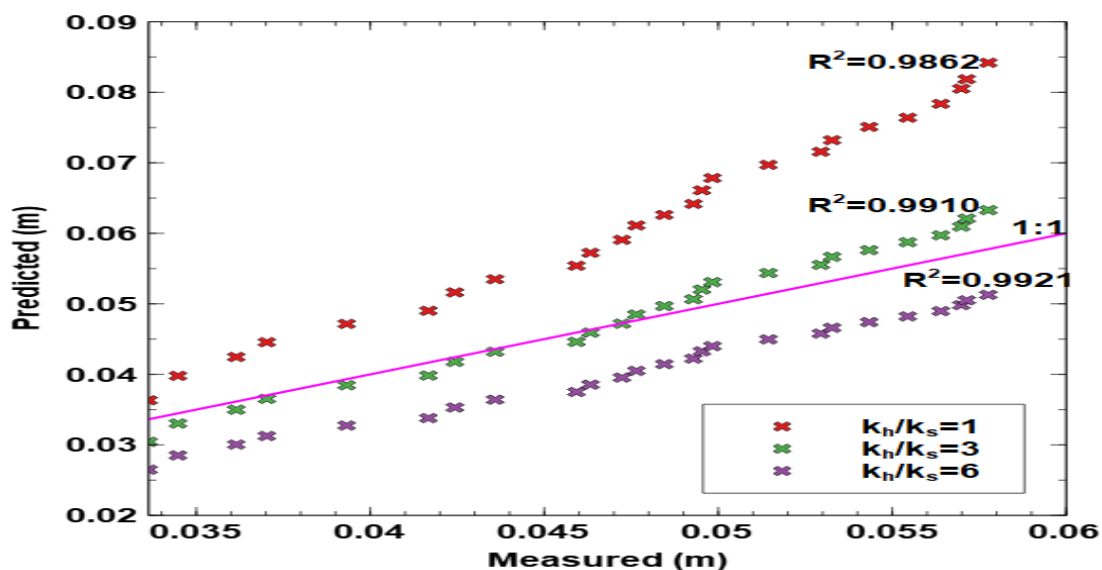


Fig. 6. The  $R^2$  values of the predicted settlement in SM 1.

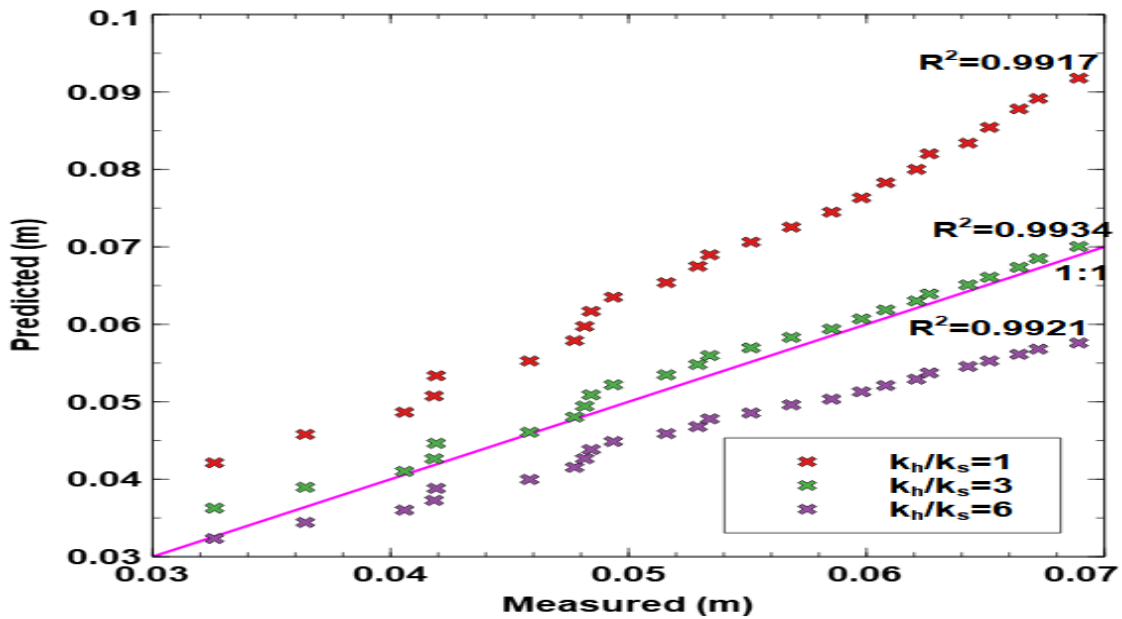


Fig. 7. The  $R^2$  values of the predicted settlement in SM 2.

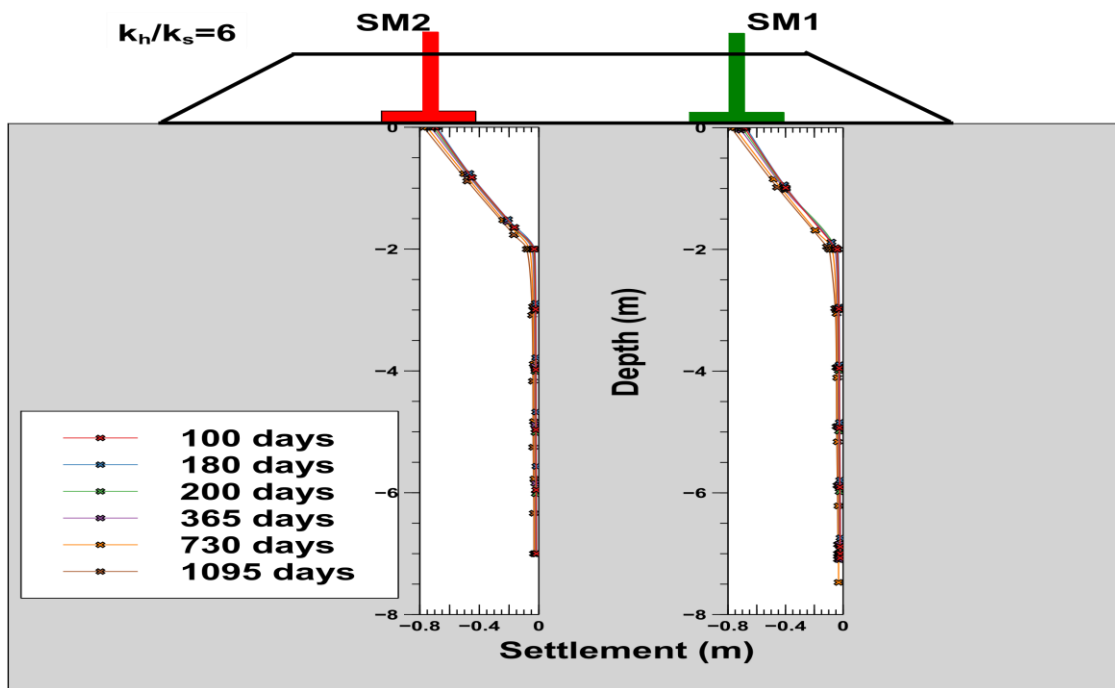


Fig. 8. Ground settlement profiles prediction.

It can also be observed that PVDs foundations were better able to maintain less pore pressure near the ground surface. Installing PVDs in soft ground speeds drainage. The excess pore water pressure inside the soil consequently diminished sharply as the PVDs progressed. If the drainage is one-way, soil consolidation occurs below the PVD site because there is

silty clay and clay silt underneath. Due to the low soil permeability and long drainage path, the excess pore water pressure under the PVDs base had to be reduced. Additionally, PN1 pore water pressure is reduced in comparison to PN2, and this may be related to the influence of the depth involved in the discharge capacity load.

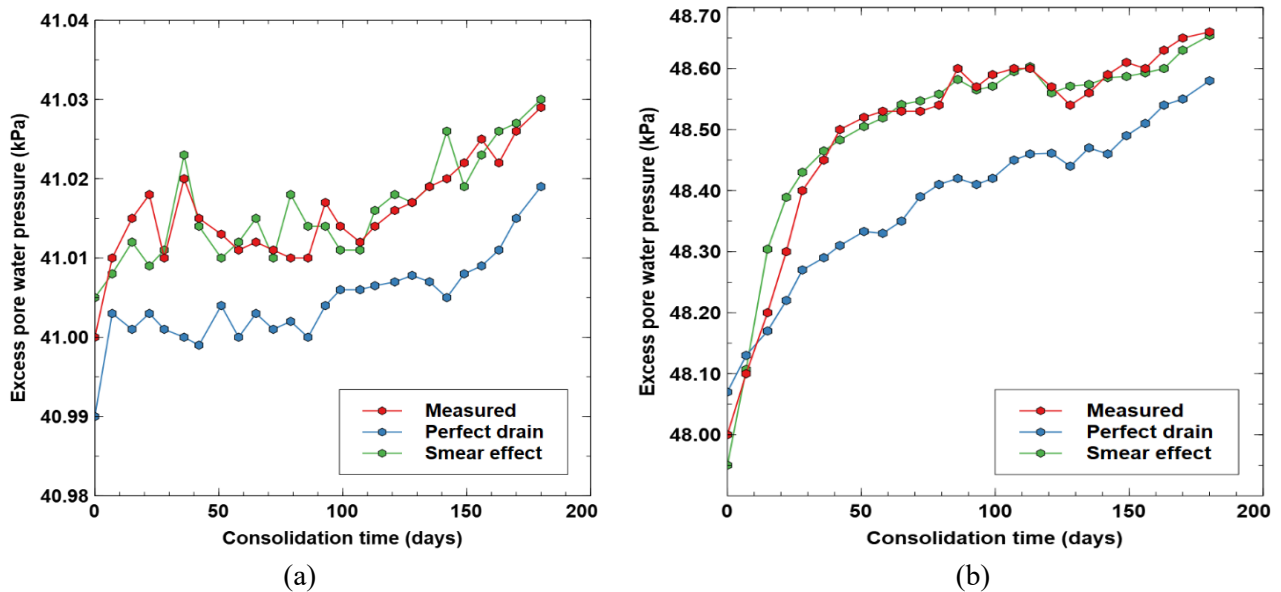


Fig. 9. Excess pore pressure variations at (a) PN1 and (b) PN2.

## 6. Conclusions

This study evaluated the performance of soft ground stabilized with PVDs beneath road embankments using a plane strain and multi-drain model of vertical drains. The numerical accuracy was evaluated by considering the smearing effect and perfect drain associated with PVDs. The inclusion of the smear effect improved the predictability of settlement and pore water pressure compared to the perfect drain. The maximum settlement was found on the ground surface, with a significant reduction occurring from the surface to a depth of 2m. The proposed approach for predicting the behaviour of PVDs improved subsoils involves evaluating the equivalent horizontal permeability and comparing predicted and measured settlements. The application of a plane strain model with a smear effect for analyzing multi-drain is proposed for future research due to its computational speed and acceptable predictive accuracy. However, the accuracy of the permeability ratio obtained

using back-calculation and finite element analysis can be affected by various factors, and careful validation against field observations is crucial.

## References

- [1] Mamat RC, Kasa A, Razali SFM. A Review of Road Embankment Stability on Soft Ground: Problems and Future Perspective. *IIUM Eng J* 2019;20:32–56. <https://doi.org/10.31436/iiumej.v20i2.996>.
- [2] Ayeldeen M, Tschuchnigg F, Thurner R. Case study on soft soil improvement using vertical drains—field measurements and numerical studies. *Arab J Geosci* 2021;14:343. <https://doi.org/10.1007/s12517-021-06701-7>.
- [3] Qi C, Li R, Gan F, Zhang W, Han H. Measurement and Simulation on Consolidation Behaviour of Soft Foundation Improved with Prefabricated Vertical Drains. *Int J Geosynth Gr Eng* 2020;6:23. <https://doi.org/10.1007/s40891-020-00208-z>.
- [4] Kjellman W. Accelerating consolidation of fine grained soils by means of cardboard wicks. *2nd Int. Conf. Soil Mech. Found. Eng., Rotterdam: 1948, p. 302–305.*

- [5] Bergado DT, Chaiyaput S, Artidteang S, Nguyen TN. Microstructures within and outside the smear zones for soft clay improvement using PVD only, Vacuum-PVD, Thermo-PVD and Thermo-Vacuum-PVD. *Geotext Geomembranes* 2021;48:828–43. <https://doi.org/10.1016/j.geotexmem.2020.07.003>.
- [6] Mamat RC, Kasa A, Mohd Razali SF. Comparative Analysis of Settlement and Pore Water Pressure of Road Embankment on Yan soft soil Treated with PVDs. *Civ Eng J* 2019;5:1609–18. <https://doi.org/10.28991/cej-2019-03091357>.
- [7] Mamat RC, Ramli A. Evolutionary polynomial regression for predicting the unconfined compressive strength of lime-stabilized. *Suranaree J Sci Technol* 2023;30:010212(1-7).
- [8] Indraratna B, Redana IW. Laboratory determination of smear zone due to vertical drain installation. *J Geotech Geoenvironmental Eng* 1998;124:180–4. [https://doi.org/10.1061/\(ASCE\)1090-0241\(1998\)124:2\(180\)](https://doi.org/10.1061/(ASCE)1090-0241(1998)124:2(180)).
- [9] Barron RA. Consolidation of fine-grained soils by drain wells. *Trans ASCE* 1948;113:718–724.
- [10] Bergado DT, Asakami H, Alfaro MC, Balasubramaniam AS. Smear effects of vertical drains on soft Bangkok clay. *J Geotech Eng* 1991;117:1509–1530. [https://doi.org/10.1061/\(ASCE\)0733-9410\(1991\)117:10\(1509\)](https://doi.org/10.1061/(ASCE)0733-9410(1991)117:10(1509)).
- [11] Mamat RC, Ramli A, Khahro SH, Yusoff NIM. Numerical Simulation and Field Measurement Validation of Road Embankment on Soft Ground Improved by Prefabricated Vertical Drains: A Comparative Study. *Appl Sci* 2022;12:8097. <https://doi.org/10.3390/app12168097>.
- [12] Indraratna B, Redana IW. Plane strain modeling of smear effects associated with vertical drains. *J Geotech Geoenvironmental Eng* 1997;123:474–478. [https://doi.org/10.1061/\(ASCE\)1090-0241\(1997\)123:5\(474\)](https://doi.org/10.1061/(ASCE)1090-0241(1997)123:5(474)).
- [13] Kamash W El, Hafez K, Zakaria M, Moubarak A. Improvement of Soft Organic Clay Soil Using Vertical Drains. *KSCE J Civ Eng* 2021;25:429–441. <https://doi.org/10.1007/s12205-020-0561-9>.
- [14] Parsa-Pajouh A, Fatahi B, Vincent P, Khabbaz H. Trial Embankment Analysis to Predict Smear Zone Characteristics Induced by Prefabricated Vertical Drain Installation. *Geotech Geol Eng* 2014;32:1187–210. <https://doi.org/10.1007/s10706-014-9789-9>.
- [15] Plaxis. Reference Manual. The Netherlands: Delft University of Technology and Plaxis b.v.; 2008.
- [16] Mamat RC, Ramli A, Samad AM, Kasa A, Razali SFM, Omar MBHC. Stability Assessment of Embankment on Soft Soil Improved with Prefabricated Vertical Drains Using Empirical and Limit Equilibrium Approaches. *Int J Adv Trends Comput Sci Eng* 2019;8:444–9. <https://doi.org/10.30534/ijatcse/2019/6481.6.2019>.
- [17] Rezanian M, Nguyen H, Zanganeh H, Taiebat M. Numerical analysis of Ballina test embankment on a soft structured clay foundation. *Comput Geotech* 2018;93:61–74. <https://doi.org/10.1016/j.compgeo.2017.05.013>.
- [18] AASHTO. Bridge Design Specifications. 6th ed. Washington, DC, US.: American Association of State Highway and Transportation Officials; 2012.
- [19] Hird CC, Pyrah IC, Russell D, Cincicoglu F. Modelling the effect of vertical drains in two-dimensional finite element analyses of embankments on soft ground. *Can Geotech J* 1995;32:795–807. <https://doi.org/10.1139/t95-077>.
- [20] Rixner JJ, Kraemer SR, Smith AD. Prefabricated vertical drains. Washington, DC, US.: 1986.
- [21] Hird CC, Moseley VJ. Model study of seepage in smear zones around vertical drains in layered soil. *Géotechnique*

2000;50:89–97.

<https://doi.org/10.1680/geot.2000.50.1.89>.

- [22] Holtz RD, Jamiolkowski M, Lancellotta R, Pedroni S. Behaviour of bent prefabricated vertical drains. 12th Int. Conf. Soil Mech. Found. Eng., vol. 3, Rio De Janeiro: 1988, p. 1657–60.
- [23] Zhang Z, Ye GB, Xu Y. Comparative analysis on performance of vertical drain improved clay deposit under vacuum or surcharge loading. *Geotext Geomembranes* 2018;46:146–54.  
<https://doi.org/10.1016/j.geotexmem.2017.11.002>.